PHARMACIA

Pharmacia 68(4): 907–917
DOI 10.3897/pharmacia.68.e71334

Research Article

Determination of TLC fingerprint biomarker of *Ipomoea batatas* (L.) Lam leaves extracted with ethanol and its potential as antihyperglycemic agent

Putu Sanna Yustiantara[1], Ni Kadek Warditiani[1], Pande Made Nova Armita Sari[1], Ni Luh Kade Arman Anita Dewi[2], Yan Ramona[3], I Made Jawi[4], I Made Agus Gelgel Wirasuta[1]

1 *Pharmacy Department, Faculty of Mathematics and Natural Science, Udayana University*
2 *Department of Natural Medicine, Faculty of Pharmacy, Universitas Mahasaraswati, Denpasar, Bali*
3 *Biology Department, Faculty of Mathematic and Natural Science, Udayana University*
4 *Biomedical Science Master Study Program, Udayana University*

Corresponding author: I Made Agus Gelgel Wirasuta (gelgel.wirasuta@unud.ac.id)

Received 9 July 2021 ♦ **Accepted** 5 October 2021 ♦ **Published** 10 December 2021

Citation: Yustiantara PS, Warditiani NK, Sari PMNA, Dewi NLKAA, Ramona Y, Jawi IM, Wirasuta IMAG (2021) Determination of TLC fingerprint biomarker of *Ipomoea batatas* (L.) Lam leaves extracted with ethanol and its potential as antihyperglycemic agent. Pharmacia 68(4): 907–917. https://doi.org/10.3897/pharmacia.68.e71334

Abstract

Antihyperglycemic activity of *Ipomoea batatas* (L.) leaves has been studied for years. As many naturally found varieties of such plant species have been used as herbal medicines, there is a need to establish a fingerprint biomarker standardization method. Our research combined TLC fingerprints and chemometric analysis to determine biomarkers in leaf ethanol extract of *Ipomoea batatas* (L.) (EIBL). We predicted the main constituents of anthocyanin glycosides and their acylated derivates in the leaf ethanol extract of such plants using ESI-MS. The EIBL that contained identified biomarkers has succeeded in providing an antihyperglycemic effect in experimental using STZ-induced rats. This study also found a linear correlation between doses of flavonoid derivates as antioxidant agents with their antihyperglycemic activities. Therefore, this biomarker information can be used as a model to predict the dose-responses of the antihyperglycemic activities produced by other leaf ethanol extracts of *I. batatas*.

Keywords

Ipomoea batatas, fingerprints, quality control, antihyperglycemic

Introduction

Ipomoea batatas (L.) has been reported to have beneficial effect by lowering blood glucose (BG) in type 2 diabetic patients (Ludvik et al. 2003, 2008, Zhao et al. 2007, Ooi and Loke 2013, Daud et al. 2016, Rafi U and Luka 2018). Indonesia has around 50 *Ipomoea batatas* (L.) cultivars (Rahajeng 2015), and among those cultivars, *Ipomoea batatas* (L.) from Bali (IBL). has been limitedly investigated. The leaves of IBL are lobed with pointed tips, young and old leaf's colors are dark purple, while the stems and leaf bones are purple. Its flower is a star-shaped flower crown, with the tip of the flower petals tapered, and the petals are pale purple. The tuber skin is purplish-white, with white flesh tuber. Tubers grow very rarely with a diameter of

1–2 cm and a length of about 5 cm in three month old plants. The leaves of IBL have been traditionally used as vegetable raw materials in traditional Balinese foods. The purple color of IBL leaf reflects its anthocyanin content. Many studies reported that anthocyanin has potential an antidiabetic agent (Matsui et al. 2002, Jayaprakasam et al. 2005, Olivas-Aguirre et al. 2016, Khoo et al. 2017, Luo et al. 2018, Al-Yousef et al. 2020, Vilhena et al. 2020). Their antihyperglycemic potency is presumed to be due to inhibition of oxidative stress, which leads to induction of pancreatic beta cells to produce sufficient insulin level (Vessal et al. 2003, Jawi et al. 2009, Pottathil et al. 2020).

Around 415 million people in 2016 worldwide were reported to suffer from diabetes and this is predicted to increase to 642 million in the next decade (Jaacks et al. 2016). Diabetes is a major cause of mortality, morbidity, and significantly increment of health care expenditures. World Health Organization recommended further investigation of herbal based medicines as antihyperglycemic agents for complementary treatments (Alqathama et al. 2020). In daily practices however, it is found that complementary medicines always contain complex compounds. Therefore, there is a need to establish standardized method in the process of raw material quality control.

Biomarker identification, also known as a quality marker (Q-marker), is necessary to ensure the safety and efficacy of herbal medicines. The phytochemical fingerprints are commonly used to identify their biomarkers. In combination with chemometric analysis, it was found useful to improve the quality control standard system of herbal medicine (Xiang et al. 2018). New herbal medicine discoveries should be accompanied by developing their standardization test method, which supports Current Good Manufacturing Practice (cGMP). The TLC fingerprint is a robust method used to identify and determine their biomarker. This study aimed to establish a TLC fingerprint method, which identified their antioxidant biomarkers of ethanolic extract of IBL leaf (EIBL), associated with antihyperglycemic activity in STZ-induced rats. The established fingerprint will be used as Q-marker on the QC/QA of cGMP in further applications.

Materials and methods

Chemicals

Citric acid, boric acid, glacial acetic acid, sulfuric acid, chloroform, ethyl ether, ferric chloride, ammonium hydroxide, ethanol 96%, methanol, and hydrochloride acid were purchased from Merck®. Phytochemical screening reagents were obtained from Merck®. Streptozotocin (STZ) was from BioWorld®, Glibenclamide, Enzymatic colorimetric method (GOD/PAP) with glucose oxidase, and 4-amino antipyrine were from Dyasis, Holzeim, Germany. All chemicals for analysis were analytical grade, except ethanol 96% for extraction was technical grade and purchased from Bratachem®, Indonesia.

Plant materials

The IBL leaves were collected from Aan Village, Klungkung Regency, Bali Province, Indonesia, and the plant was identified by *UPT Balai Konservasi Tumbuhan Kebun Raya Eka Karya* Bali-LIPI, Tabanan, Bali (voucher no 8.1303/IPH/AP/XI/2018).

Phytochemical and TLC-fingerprint authentication

Phytochemical screening

Phytochemical screening and flavonoid TLC-Fingerprint solution test was prepared by extracting 2.5 gram of the steamed IBL leaves with 25 mL of a mixture of ethanol 95% and citric acid 3% (85:15 v/v), macerated in an ultrasonic bath for 30 minutes, centrifuged at 4000 rpm, and the supernatant was transferred into a brown vial. The screening test for alkaloids, steroids/terpenoids, phenol/tannins was conducted according to the method described by Jones dan Kinghon (Jones and Kinghorn 2012). The screening test for flavonoid and saponins was conducted according to the method described in Pharmacopeia Indonesia.

Flavonoid TLC fingerprint analysis was carried out using the methods described in Harbone (1998) and Schibli and Reich (2005) with some modification (Harborne 1998, Schibli and Reich 2005). The aluminum silica gel 60 F 254 TLC plates (20x10 cm) plates were washed with ethanol and inactivated at 110 °C for 10 minutes in an oven. The EIBL previously obtained was deposited on a TLC plate at various volumes (5, 10, and 20 µL) with an automatic TLC sampler 4 (Camag-Mutten-Switzerland) fitted with a 25 µL syringe and air sprayed band. The Band length was 6 mm. The first band was applied on dimensions x = 15 mm, y = 10 mm, and with a 9.4 mm space between tracks.

The series spotted volumes were done on the different plates for intra-day and inter-day precision. The spotted samples were developed to a distance of 8 cm with mobile phase (ethyl acetate: formic acid: acetic acid: water; 100:11:11:26, v/v) in an automatic developing chamber 2 (Camag-Mutten-Switzerland) previously saturated with mobile phase vapour for 30 minutes. The developed spots were visualized under TLC-visualizer, and their image was captured under a UV lamp at wavelengths of 254 nm and 366 nm and under a white R lamp, scanned under UV light (λ 210, 330, and 543 nm absorption mode), and the *in situ* spectra of each peak were recorded. The parameter integration peak was set at the following filter factors: Savitsky-Golay 19, lowest slope, peak thresholds (minimum slope: 5, minimum height: 10 AU, minimum area: 50 AU).

For the flavonoid identification, the separated spotted on TLC plates were derived with $AlCl_3$-, ammonia vapour -, citroboric- reagents, which were carried out using the method described by Harbone (1998) (Harborne 1998), and for antioxidant markers detection used 2,2-diphenyl-1-picrylhydrazyl (DPPH) method. The spots appeared before and after derivatization were kept in a photo documentation (Camag TLC visualizer 2) and observed under white light (wl), 245 nm, and 366 nm lamp, and the images were documented with WinCat 4.10 (Camag-Mutten-Switzerland).

Detection by Mass Spectrometry (MS) was performed using TLC plate extraction. Each spot detected was scraped and washed with the same solvent during the extraction process and then injected into Electron Ionization Spray-Mass Spectrometry (ESI-MS).

TLC-fingerprint and chromatographic data processing

The authentication test begun with identification of each peak based on their level of spectrum similarity. Digital data acquisition from WinCat 4.10 output in a tabulated form contains hRf information and start, max, and end peak heights. Unaligned peaks are aligned or shifted to the same hRf-values based on the high correlation spectra ($r_{spectra} > 0.9$) and their values of peak height were arranged as rectangular data matrixes.

A multivariate statistical analysis was carried out to calculate hierarchical cluster analysis (HCA) and principal component analysis (PCA) of the matrix data set, and this was conducted with the help of Minitab 17 statistical software. The Partial Least Square (PLS) regression was applied to calculate the linear relationship between the biomarker content of samples and their measured biomarker peak areas.

Antihyperglycemic and antioxidant of IBL extract

Extract preparation

Leaves of IBL were wet sorted, 4.5 Kg were steamed in boiling water for 15 minutes, and cooled for 15 minutes. This steamed leaves were then extracted with 9 L of ethanol 95% and citric acid 3% (85:15 v/v) mixture to form pulp of IBL. The mixture were placed in a light isolated glass jar and macerated for 24 hours. The pulp was filtered using cotton cloth, the dreg was remacerated three times using the same volume of ethanol used in the first extraction, and the filtrate obtained was concentrated in a vacuum rotary evaporator.

Experimental design

Rats (30 male Wistar white rats) aged of between 6 and 8 weeks with bodyweight range of 150 – 250 grams were obtained from a local supplier (*Bikul Bali*). This research received ethical clearance from animal ethics committees (number: 2923/UN14.2.9/PD/2018). The animals were housed in an animal room at the Department of Pharmacy, Faculty of Mathematics and Natural Sciences, Udayana University, Jimbaran, Bali, Indonesia. The rats were acclimatized for seven days, and the enclosure environment was under control. These rats were divided into six groups (each containing 5 tested animals) as follows: 1) NI - No Induction (Normal Control): Given standard feed and sufficient water; 2) NT- No Treatment (Negative Control): Given standard feed, STZ (40 mg/kg BW, i.p), and sufficient water; 3) GCM - Treated with Glibenclamide 10 mg/kg (Positive Control): Given standard feed, STZ (40 mg/kg BW, i.p), glibenclamide and sufficient water; 4) EIBL.1: Given standard feed, STZ (40 mg/kg BW, i.p), extract dosage of 250 mg / BW and sufficient water; 5) EIBL.2: Given standard feed, STZ (40 mg/kg BW, i.p), extract dose of 500 mg/kg BW and sufficient water; 6) EIBL. 3: Given standard feed, STZ (40 mg/kg BW, i.p), extract dose of 750 mg/kg BW and sufficient water. The administered doses referred to total anthocyanin contained in EIBL which gave positive result on antihyperglycemic assay in previous research (Unpublished research in 2018–2019, grant number: 171.110/UN14.4.A/LT/2018 awarded to Dr. I Made Agus Gelgel Wirasuta)

Biochemical assay of Blood Glucose (BG) and Malondialdehyde (MDA)

For BG and MDA analysis, blood of rats was collected from the tail vein of fasting rats. The measurement was done before STZ induction (Pre), 72 hours after STZ induction, on days 7, 14, and 21. BG levels were measured using spectrophotometric methods. Serum previously separated from whole blood was reacted with glucose oxidase reagent (GOD/PAP). A volume of 10 µl serum sample was added into 1 mL of GOD/PAP reagent, incubated at 20–25 °C for 30 minutes, and measured for absorbance at the wavelength of 500 nm.

Measurement of MDA level in serum of rats followed the method specified by Ohkawa method (1979) (Ohkawa et al. 1979). Serum samples (amounted 100 mL) were mixed with 400 mL of 10% trichloroacetic acid (TCA) in distilled water and centrifuged at 4000 ´ g for 10 minutes. The supernatant (amounted at 500 mL) was pipetted into a new test tube, added with 1 mL of 0.67% TBA, incubated a water bath at 95 °C for 30 minutes, and cooled down to ambient temperature prior to measurement spectrophotometrically at wavelength of 532 nm.

Statistical analysis

Data of Blood Glucose (BG) and malondialdehyde (MDA) levels were statistically analyzed for homogeneity and normality, distribution of data, and Mann-Whitney test, with the help of SPSS version 24 for windows at $p < 0.05$. Correlation analysis was calculated and visualized as a matrix using the stats package in R programming software (R Core Team 2019). The relationship between BG and MDA levels was calculated using Spearman correlation test.

Results and discussion

Phytochemical and TLC-fingerprint Authentication

The phytochemical screening tests showed that the plant extract gave positive reaction for flavonoid, saponin, tannin, phenol, and triterpenoid tests, but negative for alkaloid test. TLC images of the sample following elution with mobile phase before and after derivatization, dendrogram after scanning at 210 nm, and the *in situ* UV-vis spectra of detected peaks are presented in Figures 1a, 1b, and 1c, respectively. The flavonoid identification which was based on

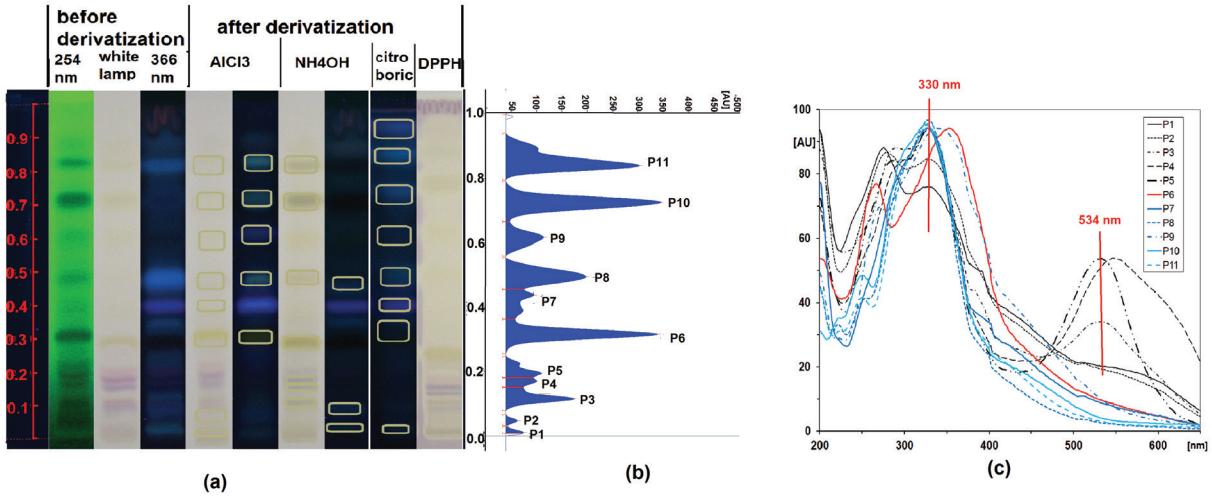

Figure 1. TLC profile of EIBL after eluted with flavonoid mobile phase. **a**) Derivatized TLC plate, **b**) densitogram, and **c**) spectra of detected peaks.

Table 1. Identification flavonoid content in ethanolic EIBL. wl: white lamp; qs: quenching; fl: fluorescence.

Peak	Bxefore derivatization				After derivatization						Assigned flavonoid present
	Rf max	254 nm	wl	366 nm	$AlCl_3$ (wl)	$AlCl_3$ (366 nm)	NH_4OH (wl)	NH_4OH (366 nm)	Citro boric (366 nm)	DPPH (wl)	
P1	0.01	qs	dull orange	yellow fl	yellow	–	dull blue	dull yellow fl	dull yellow fl	+	Anthocyanin
P2	0.05	qs	dull orange	yellow fl	yellow	–	dull blue	dull yellow fl		+	Anthocyanin
P3	0.12	qs	red –violete	yellow fl	–	–	blue	–		+	Anthocyanin
P4	0.17	qs	red – violete	yellow fl	–	–	blue	–		+	Anthocyanin
P5	0.19	qs	mauve	yellow fl	–	–	blue	dull yellow fl	yellow fl	+	Anthocyanin
P6	0.32	qs	dull yelow	yellow fl	yellow	yellow fl	yellowish blue	dull yellow fl	yellow fl	+	Flovonol/ Flavones
P7	0.44	qs	dull yellow	blue fl	dull yellow	blue fl	–	–	blue fl	+	Flavonol/ Flavones
P8	0.49	qs	dull yellow	blue fl	dull yellow	yellow fl	yellowish blue	–	yellow fl	+	Flavonol/ Flavones
P9	0.62	qs	dull yellow	dull yellow fl	dull yellow	yellow fl	–	–	yellow fl	+	Flavonol/ Flavones
P10	0.73	qs	yellow	yellow fl	dull yellow	yellow fl	blue	–	yellow fl	+	Flavonol/ Flavones
P11	0.84	qs	dull yellow	dull yellow fl	dull yellow	yellow fl	blue	–	yellow fl	+	Flavonol/ Flavones

derivatization reagent results and their *in situ* spectra are presented in Table 1. Peaks in P1–P5 are presented as dull orange – violet – mauve. These colors usually represent anthocyanin, while peaks P6–P11 indicated the presence of flavonol or flavon (Markham 1989). Yellow bands on purple background following spraying with DPPH reagent indicated positive reactions with DPPH. All peaks showed this phenomenon, indicating that they have potential as agents of electron scavenging antioxidants.

Flavonoids are characterized by a high absorbance at the wavelength of between UV 250–270 nm, while anthocyanins produce a high visible spectra area between 460 - 550 nm as part of their color characteristics. The color intensity is caused by a positive charge on the structure of the flavylium (Delgado-Vargas et al. 2010). In this study, the structural diversity of flavonoid and anthocyanin derivatives is a distinguishing factor in λ_{max} of UV-Vis spectra. In previous studies, the aglycon, glycoside, and acylated structure of flavonoids were reported to have an impact on shifting λ_{max} UV-Vis spectra (Giusti and Wrolstad 2003). The methoxy in flavylium and acylated anthocyanins are reported to be stable on increasing pH conditions (Delgado-Vargas et al. 2010, Song et al. 2013, Khoo et al. 2017, Favaro et al. 2018). The difference in maximum wavelength is an indication of the diversity of glucosides and acylated in EIBL.

The peaks on the chromatogram as a fingerprint marker were tested for precision with several variations in the volume of the intraday markers (Fig. 2). The difference in Rf values during separation using TLC has potential of misinterpretation in the authentication of Q-marker compounds. To fix this problem, fine-tuning the data by shifting based on the similarity *in situ* spectra was applied. The separation results of the eleven peaks identified before and after fine-tuning are shown in Figure 2 a-1 and Figure 2 a-2, respectively. The peaks with high correlation spectra ($r_{spectra} > 0.9$) are registered as the same peak and created in a "Gram-matrix" (Daszykowski et al. 2008). This approach succeeded in providing a better clustering pattern in cluster analysis by optimizing the covariance between peak variables (Fig. 2 b-1, and b-2). In a comparison of the level of similarity, the original data has only 34.59% similarity among samples, while the fine-tuned dataset has succeeded in producing similarity of up to 98.42%. This approach can minimize variation caused by technical errors during the experiment.

Peak misalignment in chromatography is not a new issue related to its application in multivariate analysis. Moreover, in its technical application, a fine-tuning chromatography dataset in TLC has challenges when applied to samples of natural products which have limited reference compounds

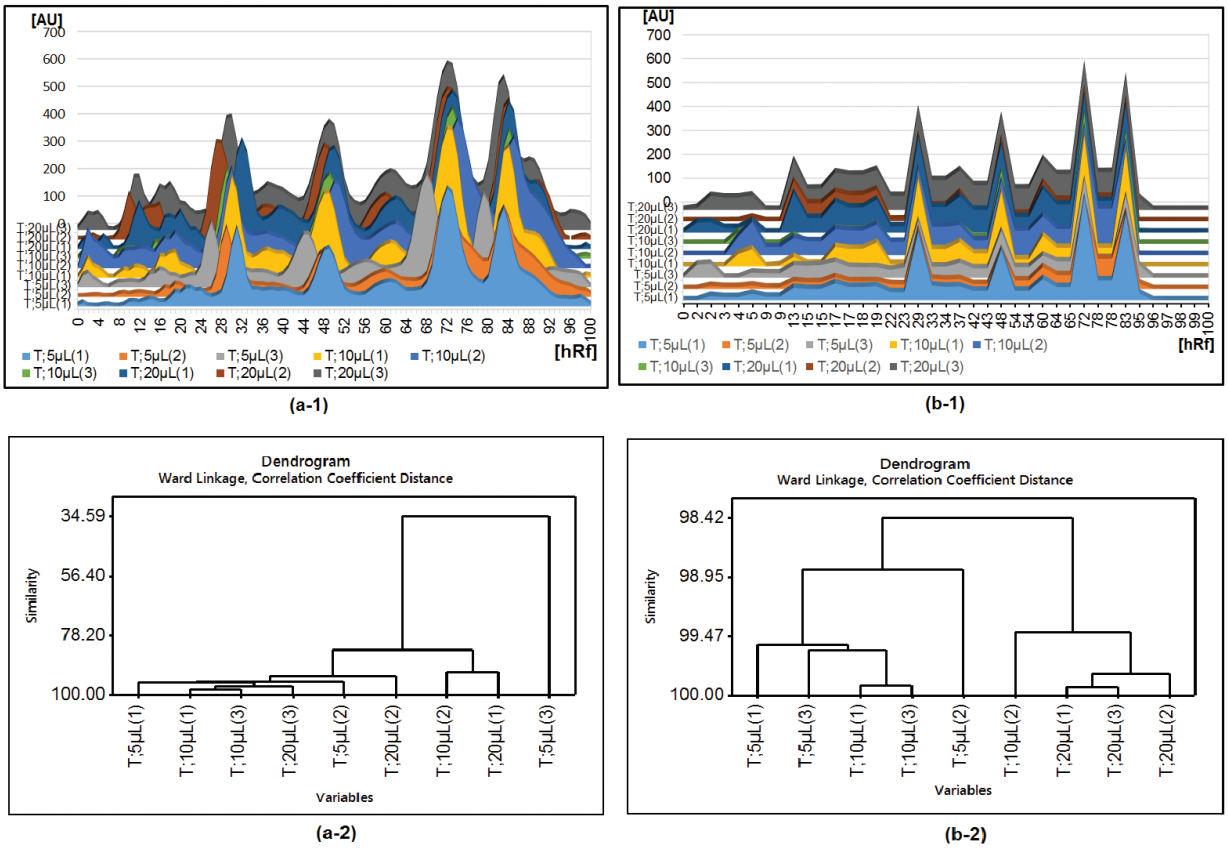

Figure 2. TLC intra-day precision of EIBL. **a**) Without peak shifting and **b**) with peak shifting.

(Komsta 2012). This problem also becomes a limitation in using the automatic warping method in TLC. In this study therefore, signal spectra were used as a marker of similarity in constructing the matrix chromatogram data to overcome this limitation. Time consumption may be a consideration of this approach. However, with the current sophisticated software technology of TLC-densitometer, correlation calculations and registers for each peak or separate compound can be done *in situ* on WinCat (version 4.10).

Presumed anthocyanin derivates (Peaks P1–P5) and flavonols/flavones (Peaks P6–P11) were scanned in two different wavelengths (330 nm and 543 nm), several peaks in high peak area values at each wavelength (Fig. 3 a-1 and b-1). Based on the antioxidant activity in the DPPH test (Fig. 1a), the application of single λ_{max} is insufficient in representing the quantity of the identified bioactive compound. Therefore, selected λ_{max} (330 nm and 543 nm) was applied to construct a combined dataset for the multivariate analysis. First of all, the combined dataset of the IBL biomarker is validated using PLS (Fig. 3 c-1). In PLS modelling, the multicollinearity of each peak height of the precision sample was calculated based on spotting volume. PLS produces a linear correlation between the calculated response and the actual response, which represents the combined dataset maintaining a high correlation between samples. Thereafter, the PCA score plot is used to observe the contribution of each variable, which are the bioactive peaks based on the variation of spotting volume. Their contribution is described as a coordinate point (Fig. 3 a-2, b-2, c-2), where the low AUC peaks gather in one area when analyzed using a single wavelength. In contrast, the combined dataset produces a spread contribution of the PCA score plot. The results indicate that the combination of wavelengths can be used in an assessment of bioactive quality control (Q-marker), such as an antioxidant in IBL.

Eleven peaks in TLC of EIBL were identified by ESI-MS using indirect technique (Table 2). Predictable derivatives of flavonoids and anthocyanins include Peonidin-caffeoyl-p-hydroxybenzoylsophorside-5-glucoside (P2), pelargonidin glucoside or cyanidin 3-O-rutinoside (P8), peonidin dirhamnosaloyl-glucoside isomer, or cyanidin-3-glucoside isomer. (P9), cyanidin 3-O-rutinoside (P10), and peonidin dirhamnoside (P13). We also noted a consistent fragmentation pattern at 701.6 m/z (P2, P4, P5, and P7), which indicates the possibility to be assigned as peonidin derivative (P2). The results of the ESI-MS identification consisted of two distinct groups, namely high and low molecular weight compounds. The high molecular weight (P1–P7) of the parent ion is obtained in positive ionization between 1120 to 1348 *m/z*, while the low molecular weight (P8–11) is obtained in positive ionization between 593 to 595 *m/z*. High *m/z* in anthocyanins indicates a complex structure of glucosides and acylated anthocyanins molecules, while compounds with positive ionization of lower than 590 m/z are predicted to be anthocyanins glycoside.

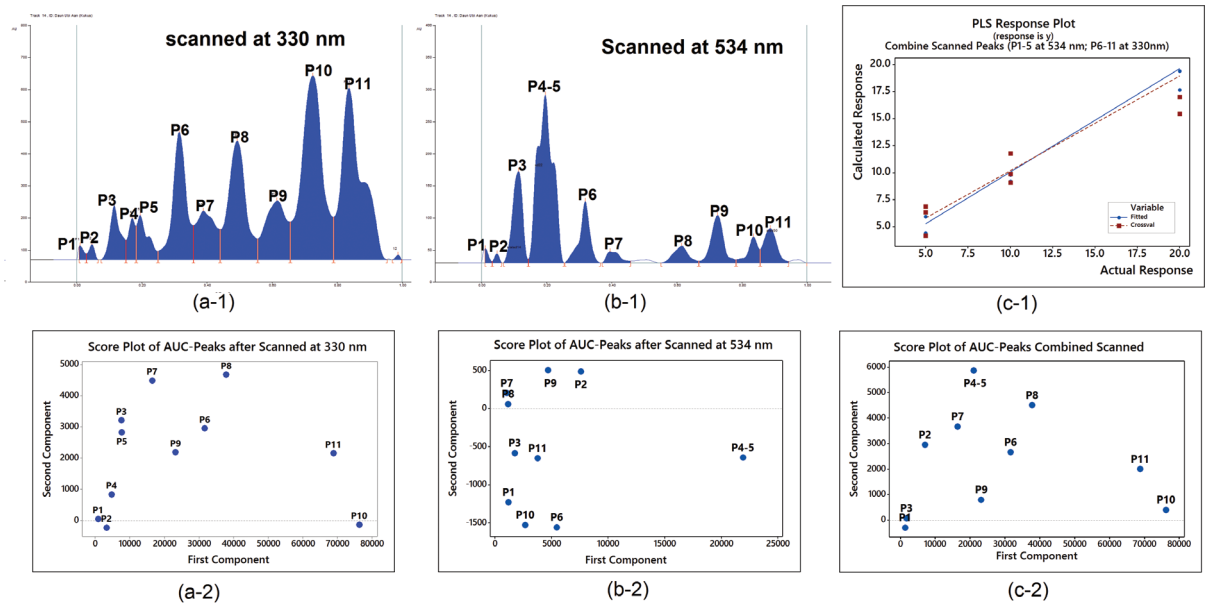

Figure 3. Densitogram and chemometric fingerprint of EIBL scanned in **a-1**) 330 nm and **b-1**) 534 nm; **c-1**). Response plot after the AUC-peaks dataset combined and trained in PLS; PCA score plot of AUC-peaks dataset in (**a-2**) 330 nm, (**b-2**) 534 nm and (**c-2**) combined dataset.

Table 2. Predicted compounds found in EIBL using ESI-MS compared to available reference. * predicted derivatives based on fragmentation similarity.

Peak number	[m/z]		Predicted compound (Reference)
	MH^+	Other fragmentation	
1	1120.7	930.5, 843.4, 747.6, 703.7, 663.4, ***633.5***	n.d
2	1170.4	814.5, 775.6, 755.6, ***701.6***, 678.2, 601.8	Peonidin 3-caffeoyl-*p*-hydroxybenzoylsophorside-5-glucoside (Sun et al. 2018, Li et al. 2019, de Jesus et al. 2021)
3	1360.3	815.1, 792.5, 749.2, ***702.7***, 657.6, 607.2	n.d.
4	1237.4	937.3, 831.4, ***701.6***, 650.5, 620.9	Peonidin derivates*
5	1319.2	1275.8, 1195.5, 792.7, 724.1, ***701.6***, 641.0	Peonidin derivates*
6	1348.1	814.2, 792.4, 725.2, ***680.6***, 631.9	n.d.
7	1348.8	814.6, 793.5, 750.0, ***701.6***, 646.9, 609.8	Peonidin derivates*
8	595.2	576.1, 563.9, 532.2, 510.0, 492.1, 451.6, 435.3, 420.5, 397.4, 376.5, 361.4, 328.1, 309.6, 288.2, ***279.3***, 266.4	Pelargonidin-3,5-diglucoside (Lopes-Da-Silva et al. 2002) / Cyanidin3-O-rutinoside(Kim and Lee 2020)
9	593.7	585.1, 567.2, 540.6, 531.9, 510.4, 497.1, 456.1, 413.8, 367.0, 340.8, 321.3, 307.2, 294.3, ***275.***9, 260.1	Peonidin dirhamnoside isomer (Al-Yousef et al. 2020) / Cyanidin-3-dioxaloyl-glucoside (Olivas-Aguirre et al. 2016)
10	594.9	571.2, 540.0, 519.0, 516.7, 432.9, 398.1, 391.2, 374.9, 340.5, 333.0, 315.9, 294.0, ***276.1***, 260.2	Cyanidin 3-O-rutinoside (Lopes-Da-Silva et al. 2002, Kim and Lee 2020)
11	593.4	587.3, 568.8, 540.6, 530.2, 510.2, 481.6, ***453.4***, 443.3, 412.9, 397.6, 384.6, 349.7, 306.4, 272.5, 252.1	Peonidin dirhamnoside (Al-Yousef et al. 2020)

Several studies reported that anthocyanins losing their functional flavylium chromophore after donating protons at a high pH (pH>3) (Coutinho et al. 2015, Khoo et al. 2017, Favaro et al. 2018). This study was performed at pH 3, where most of the anthocyanins tend to be stable. Hence, that information about the spectral discrepancies and mass spectrometry observed is possible due to the various structural complexity of the metabolites contained therein. As a preliminary assumption, the flavonoid derivatives found in EIBL are primarily anthocyanins and have been shown to have potential as electron scavenging antioxidant agents. The identification of EIBL flavonoid derivates and anthocyanins using TLC can be considered for its application in quality control, especially in measuring the relative quantity of substances that will affect the pharmacological response.

Antihyperglycemic and antioxidant effect of IBL extract

Antihyperglycemic and antioxidant activity of ethanolic Extract of IBL leaf (EIBL) were successfully tested using STZ induction procedures in male Wistar white rats. Three types of controls were included during the experiment, namely: (1) normal control group showing the condition of the rats without induction, (2) positive control group using glibenclamide (GCM) which was thought to be able to reduce BG and maintain MDA levels at low levels, and (3) negative control group that gave diabetic condition characterized by high levels of BG and MDA after induction. EIBL dosage variations were used to determine the effect of dose on response.

STZ induction for three consecutive days was successful to increase BG level due to insulin deficiency. STZ is a glucose analogue with selective affinity for the pancreatic beta-cell GLUT-2 (Glucose Transporter-2) receptor (Szkudelski 2001). An increase in blood sugar level due damages of pancreatic beta cells may result in permanent inability of these cells to produce insulin. STZ stimulates oxidative stress by enhancing nitric oxide (NO) level and

generating free radical molecules in beta cells (Akiyama et al. 2001, Szkudelski 2001, Lenzen 2008). GMC was found to be effective to decrease blood glucose levels after induction. The role of GMC is to stimulate insulin secretion by pancreatic beta cells, and this ensure sufficient glucose uptake into cells. GMC was also reported to inhibit the initiation of lipid peroxide (LPO) formation when insufficient uptake occurred (Erejuwa et al. 2010, Rabbani et al. 2010, Obi et al. 2015, Pandarekandy et al. 2017, Pottathil et al. 2020). Enhancement of lipid peroxide (LPO) was monitored through MDA as its main product.

The BG level in each group was monitored at the time intervals shown in Figure 4a. Before induction, statistical analysis of BG showed no significant difference in all groups, indicating that all tested animals had similar BG level and eligible to be included in the tests. After induction (D0, 72 hours after STZ induction), NI increased significantly ($p < 0.05$, Mann-Whitney test) when compared to the other groups, and this was due to STZ induction. BG levels decreased significantly in EIBL groups on the seventh day after induction ($p > 0.05$, Mann-Whitney test). The BG levels of all EIBL groups and the NI group were observed to be stable at comparable levels, and these were not significantly different from day 7 to day 21. The correlation between groups in responding to glycemic condition is presented in the matrix plot (Fig. 4b). High correlation ($r > 0.8$, $p < 0.001$) was obtained among all EIBL groups. Compared with the GCM group, the more the increasing dose of EIBL, the higher the correlation ($r_{EIBL.3} > r_{EIBL.2} > r_{EIBL1}$; $p < 0.001$ for all). Furthermore, a very low correlation was obtained in the NI ($r < 0.12$) and NT ($r < 0.14$) control group. These results suggested antihyperglycemic activity of EIBL.

The values of MDA levels in each group were monitored and the results are shown in Figure 4c. Before induction, no difference in MDA levels was found in all groups, indicating that oxidative stress has not occurred at this time. After STZ induction, a significant increase in MDA levels ($p < 0.05$, Mann-Whitney test) was observed in all induced groups, while in the NI group the values remained around normal levels. On days 7, 14, and 21, the level of oxidative stress increased significantly in the NT group. Meanwhile, MDA levels fell consistently from day 7 to day 21 in the treatment group. Administration of both GCM and EIBL reduced the level of oxidative stress to normal levels following induction. The correlation between groups of oxidative stress levels of induced rats are shown in the matrix plot in Figure 4.d. Mid to high correlations of MDA levels were obtained among EIBL.1, EIBL.2 and EIBL.3 ($r = 0.65$, $p < 0.001$; $r = 0.56$, $p < 0.01$; and 0.75 $p < 0.001$, respectively). Furthermore, a weak correlation was observed in the NI ($r < 0.21$) and NT ($r < 0.14$) groups when compared with the treatment groups. EIBL.1 and EIBL.2 were strongly correlated with the GCM group ($r = 0.85$ and $r = 0.81$, respectively, $p < 0.001$ for both) while higher dose at EIBL.3 reduced the correlation between them ($r = 0.59$, $p < 0.01$). The similarity in the rate of reduction in MDA levels between the GCM and EIBL groups showed comparable activity in preventing the increase in oxidative stress after STZ induction. However, in EIBL, the rate of reduction is likely influenced by the dose of administration.

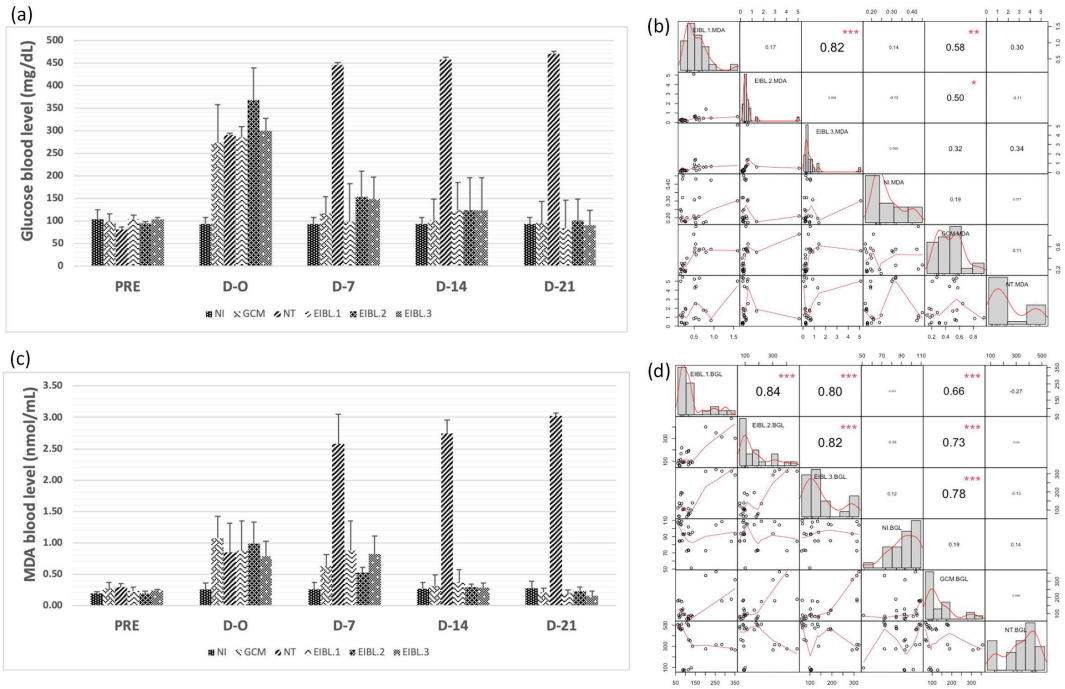

Figure 4. (**a**) Blood glucose levels of rats; (**b**) Group dosage-glucose response correlation; (**c**) MDA levels in rats; (**d**) Group dosage-MDA response correlation. Pre: blood glucose levels before STZ administration; D-0: blood glucose level 72 hours after STZ loading; D-7: blood glucose levels 7 days after treatment; D-14: blood glucose levels 14 days after treatment; D-21: blood glucose levels 21 days after treatment; * $p < 0.05$; ** $p < 0.01$; *** $p < 0.001$.

The relationship between BG and MDA levels was analyzed using the Spearman correlation test to obtain information on the available data (Fig. 5). The first analysis was aimed to determine the correlation at the induction and monitoring stage. Before induction, BG and MDA levels showed random point correlation, indicating normal conditions depending on the biological condition of each rat. After 72 hours of induction (D0), the correlation turned positive with a mid-linearity level (r_{D0} = 0.56, p = 0.0014) which is a sign both of BG and MDA levels increasing at the same time. To observe the relationship among monitoring days, the NI group data were omitted to prevent bias in the analysis. Seven days after induction, BG and MDA level shows low correlation (r_{D7} = 0.29, p = 0.15), then increased on day-14 (r_{D14} = 0.45, p = 0.021), and a high correlation was found on monitoring day-21 (r_{D21}) = 0.72, p <0.001). The second analysis was aimed to determine the correlation in each group. The NI group had a negative correlation between BG and MDA levels, while all induced groups resulted in a positive correlation. All EIBL groups produced a positive correlation value with EIBL.1 and the correlation level was medium ($r_{EIBL.1}$= 0.42, p = 0.035) while EIBL.2 produce a comparable correlation level to GCM ($r_{EIBL.2}$= 0.75 and r_{GCM} = 0.72 with p < 0.001 for both). Increasing the dose at EIBL.3 decreased the correlation of BG and MDA levels ($r_{EIBL.3}$= 0.6, p <0.0016).

EIBL groups did not cause a significant reduction in BG after seven days of STZ induction. In addition, increasing the dose resulted in a decrease in BG levels at all monitoring times. In contrast to the MDA level, high doses and long duration of administration of EIBL produce more reduction in oxidative stress. This activity indicates the dose and time-dependent mechanism of EIBL as an antioxidant. The correlation between BG and MDA is an insight in explaining the characteristics of EIBL activities. The strongest correlation was obtained in EIBL.2, which means that 500 mg/kg administration is the best-fit dose to explain the relationship between potential oxidative protection and hyperglycemic conditions. The dose of 250 mg/kg EIBL was only partially correlated, while 750 mg/kg of EIBL produced a slightly decreased relationship between BG and MDA. The lowering in BG tended to be stagnant after seven days, and on the other hand, the MDA levels decreased in a gradient on days 7, 14, and 21 after the administration of EIBL. Moreover, statistical results per monitoring day show that the maximum correlation in this study is after 21 days. It suggested that EIBL activity tends to protect against oxidative damage to STZ-induced rat pancreatic beta cells. Gradual oxidative stress levels recovery (back to normal conditions) was due to the antioxidant activity of EIBL. Eventually, beta cells are maintained in numbers to produce enough insulin, and BG levels are controlled at a low level from the beginning of treatment. Protection of pancreatic beta-cell islets was also reported after administration of antioxidant agents through inhibition of intracellular reactive oxygen species (ROS) and nitric oxide (NO) scavenging mechanisms (Szkudelski 2001, Vessal et al. 2003). ROS

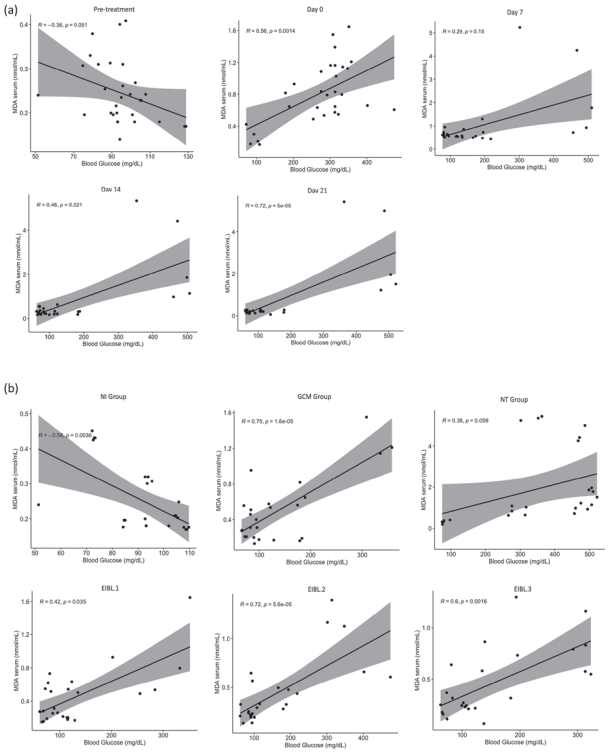

Figure 5. Relationship between oxidative stress and glycemic level in STZ-induced rats. (**a**) BG-MDA correlation level on the monitoring stage (NI group data were omitted on days 7, 14, and 21); (**b**) BG-MDA correlation level on each group.

and NO play important role in the formation of auto-poly (ADP-ribosylation) from PARP, which inhibits the *reg* gene transcription complex, causing termination of the beta-cell (Akiyama et al. 2001, Szkudelski 2001). Furthermore, the study also reported that the rate of cell regeneration increased with increasing doses of the administered antioxidants (Vessal et al. 2003), which is in line with the findings of our study.

The main anthocyanin aglycones in *I. batatas* leaves are cyanidin and peonidin (Islam et al. 2002, Li et al. 2019). Likewise, in EIBL, cyanidin and peonidin aglycone were also found, dominating the glycosides and their acylated derivatives. There was limited information on pelargonidin content in *I. batatas* leaves, yet, negligible amounts found in tuber root (Truong et al. 2010). Peonidin-caffeoyl-feruloyl-sophoroside-5-glucoside, a peonidin derivate is commonly found in *I. batatas*. This molecule shows glycemic control through inhibition of maltase-glucoamylase (MGAM) in the small intestinal rats (Matsui et al. 2002). Inhibition of sugar absorption in the intestine can control the amount of sugar in the blood, and then glucose uptake in cells is fulfilled and protected from autooxidation. Cyanidin-3-Rutinoside was reported to reduce blood glucose levels by inhibiting carbohydrate absorption in the intestine by α-glucosidase inhibition mechanism (Adisakwattana, Sirichai, Sirintorn Yibchok-Anun, Piyawan Charoenlertkul 2011). Pelargonidin and its derivates have been reported to stimulate insulin secretion. Pelargonidin aglycones increased secretion insulin up to 1.4 fold

while its glycoside (pelargonidin-3-galactoside) failed to induce insulin secretion (Jayaprakasam et al. 2005).

Antioxidant activity of anthocyanins was reported to be related to the phenolic hydroxyl in the B-ring aglycone found in cyanidin and peonidin (Luo et al. 2018). In addition, that antioxidant activity increased with the addition of phenolic to the acylated residue (Németh et al. 2003, Khoo et al. 2017, Luo et al. 2018, Al-Yousef et al. 2020). Anthocyanins with aglycon cyanidin and acylated caffeoyl residue have higher antioxidant activity due to the catechol structure, namely the diphenol structure, which is more potent in donating electrons to LPO radicals (Luo et al. 2018). Acylation in anthocyanins provides more stability in the structure, but their absorption ability was limited by its large molecular size (Fang 2014). Based on these aforementioned studies, it is suggested that EIBL maintain blood sugar levels by preventing the absorption of excess sugar from the digestive tract and the aglycons successfully absorbed will protect pancreatic beta cells.

Conclusion

This study demonstrated the use of TLC fingerprints to determine biomarker compounds in leaf ethanol extract of IBL (EIBL). The main flavonoid derivative compounds identified in this study were anthocyanins and their acylated form. Linear correlation of selected λ_{max} of antioxidant biomarker was determined from multivariate analysis. The EIBL has antihyperglycemic activity in STZ-induced rats. This pharmacological activity was due to flavonoids as agent of antioxidants. Linear correlation between the dose of flavonoid antioxidant agents and the antihyperglycemic activity was demonstrated in our study. The antihyperglycemic effect of flavonoid antioxidant agents showed a positive correlation to glibenclamide. This study indicated that the selected biomarker could be used as Q-marker on the QC/QA of cGMP process control. Those Q-markers can be used to describe the relationship between dose-response and the antihyperglycemic activity of EIBL.

References

Adisakwattana S, Yibchok-Anun S, Charoenlertkul P, Wongsasiripat N (2011) Cyanidin_3_rutinoside alleviates postprandial hyperglycemia and its synergism with acarbose by inhibition of intestinal α_glucosidase. Journal of Clinical Biochemistry and Nutrition 49(1): 36–41.

Akiyama T, Takasawa S, Nata K, Kobayashi S, Abe M, Shervani NJ, Ikeda T, Nakagawa K, Unno M, Matsuno S, Okamoto H (2001) Activation of Reg gene, a gene for insulin-producing-cell regeneration: Poly(ADP-ribose) polymerase binds Reg promoter and regulates the transcription by autopoly(ADP-ribosyl)ation. Proceedings of the National Academy of Sciences 98: 48–53. https://doi.org/10.1073/pnas.98.1.48

Al-Yousef HM, Hassan WHB, Abdelaziz S, Amina M, Adel R, El-Sayed MA (2020) UPLC-ESI-MS/MS Profile and Antioxidant, Cytotoxic, Antidiabetic, and Antiobesity Activities of the Aqueous Extracts of Three Different Hibiscus Species. Journal of Chemistry 2020: e 6749176. https://doi.org/10.1155/2020/6749176

Alqathama A, Alluhiabi G, Baghdadi H, Aljahani L, Khan O, Jabal S, Makkawi S, Alhomoud F (2020) Herbal medicine from the perspective of type II diabetic patients and physicians: what is the relationship? BMC Complementary Medicine and Therapies 20: 65. https://doi.org/10.1186/s12906-020-2854-4

Coutinho IB, Freitas A, Maçanita AL, Lima JC (2015) Effect of water content on the acid-base equilibrium of cyanidin-3-glucoside. Food Chemistry 172: 476–480. https://doi.org/10.1016/j.foodchem.2014.09.060

Daszykowski M, Danielsson R, Walczak B (2008) No-alignment-strategies for exploring a set of two-way data tables obtained from capillary electrophoresis – mass spectrometry. Journal of Chromatography A 1192(1): 157–165. https://doi.org/10.1016/j.chroma.2008.03.027

Daud N, Rosidah, Nasution MP (2016) Antidiabetic activity of *Ipomoea batatas* L. leaves extract in streptozotocin-induced diabetic mice. International Journal of PharmTech Research 9(3):167–70.

Delgado-Vargas F, Jimenez AR, Paredes-Lopez O (2010) Critical Reviews in Food Science and Nutrition, 40:3 Critical Reviews in Food Science and Nutrition. Natural Pigments: Carotenoids, Anthocyanins, and Betalains – Characteristics, Biosynthesis, Processing, and Stability. Critical Reviews in Food Science and Nutrition 40(3): 173–289. https://doi.org/10.1080/10408690091189257

Erejuwa OO, Sulaiman SA, Wahab MSA, Sirajudeen KNS, Md Salleh MS, Gurtu S (2010) Antioxidant protective effect of glibenclamide and metformin in combination with honey in pancreas of streptozotocin- induced diabetic rats. International Journal of Molecular Sciences 11: 2056–2066. https://doi.org/10.3390/ijms11052056

Fang J (2014) Bioavailability of anthocyanins. Drug Metabolism Reviews 46: 508–520. https://doi.org/10.3109/03602532.2014.978080

Favaro LIL, Balcão VM, Rocha LKH, Silva EC, Oliveira JM, Vila MMDC, Tubino M (2018) Physicochemical characterization of a crude anthocyanin extract from the fruits of jussara (Euterpe edulis Martius): Potential for food and pharmaceutical applications. Journal of the Brazilian Chemical Society 29: 2072–2088.

Giusti MM, Wrolstad RE (2003) Acylated anthocyanins from edible sources and their applications in food systems. Biochemical Engineering Journal 14: 217–225. https://doi.org/10.1016/S1369-703X(02)00221-8

Harborne JB (1998) Phytochemical Methods A Guide To Modern Tecniques Of Plant Analysis, Third Edition. Chapman & Hall, 58.

Islam MS, Yoshimoto M, Terahara N, Yamakawa O (2002) Anthocyanin compositions in sweetpotato (*Ipomoea batatas* L.) leaves. Bioscience, Biotechnology and Biochemistry 66: 2483–2486. https://doi.org/10.1271/bbb.66.2483

Jaacks LM, Siegel KR, Gujral UP, Narayan KMV (2016) Type 2 diabetes: A 21st century epidemic. Best Practice and Research: Clinical Endocrinology and Metabolism. https://doi.org/10.1016/j.beem.2016.05.003

Jawi IM, Arijana IN, Subawa A, Wirasuta IM (2009) The pharmacological mechanisms of Anthocyanin in Aqueous Extract of Purple Sweet Potato as Antihyperglycemic Herbal Remedy. Current opinion in investigational drugs (London, England : 2000).

Jayaprakasam B, Vareed SK, Olson LK, Nair MG (2005) Insulin secretion by bioactive anthocyanins and anthocyanidins present in fruits. Journal of Agricultural and Food Chemistry 53: 28–31. https://doi.org/10.1021/jf049018+

de Jesus MSC, Santiago MCP de A, Pacheco S, Gouvêa ACMS, Nascimento L da S de M do, Borguini RG, Guerra JGM, Espindola JAA, Godoy RL de O (2021) Acylated anthocyanins from organic purple-fleshed sweet potato (*Ipomoea batatas* (L.) lam) produced in Brazil. Scientia Agricola 78: 1–9. https://doi.org/10.1590/1678-992x-2019-0309

Jones WP, Kinghorn AD (2012) Extraction of Plant Secondary Metabolites BT - Natural Products Isolation. In: Methods in Molecular Biology (Methods and Protocols). https://doi.org/10.1007/978-1-61779-624-1_13

Khoo HE, Azlan A, Tang ST, Lim SM (2017) 61 Food and Nutrition Research Anthocyanidins and anthocyanins: Colored pigments as food, pharmaceutical ingredients, and the potential health benefits. https://doi.org/10.1080/16546628.2017.1361779

Kim I, Lee J (2020) Variations in anthocyanin profiles and antioxidant activity of 12 genotypes of mulberry (Morus spp.) fruits and their changes during processing. Antioxidants 9. https://doi.org/10.3390/antiox9030242

Komsta Ł (2012) Chemometrics in Fingerprinting by Means of Thin Layer Chromatography. Chromatography Research International 2012: 1–5. https://doi.org/10.1155/2012/893246

Lenzen S (2008) The mechanisms of alloxan- and streptozotocin-induced diabetes. Diabetologia 51: 216–226. https://doi.org/10.1007/s00125-007-0886-7

Li GL, Lin Z, Zhang H, Liu Z, Xu Y, Xu G, Li H, Ji R, Luo W, Qiu Y, Qiu S, Tang H (2019) Anthocyanin Accumulation in the Leaves of the purple sweet potato (*Ipomoea batatas* L.) Cultivars. Molecules 24. https://doi.org/10.3390/molecules24203743

Lopes-Da-Silva F, De Pascual-Teresa S, Rivas-Gonzalo J, Santos-Buelga C (2002) Identification of anthocyanin pigments in strawberry (cv Camarosa) by LC using DAD and ESI-MS detection. European Food Research and Technology 214: 248–253. https://doi.org/10.1007/s00217-001-0434-5

Ludvik B, Hanefeld M, Pacini M (2008) Improved metabolic control by *Ipomoea batatas* (Caiapo) is associated with increased adiponectin and decreased fibrinogen levels in type 2 diabetic subjects. Diabetes, Obesity and Metabolism. https://doi.org/10.1111/j.1463-1326.2007.00752.x

Ludvik B, Waldhäusl W, Prager R, Kautzky-Willer A, Pacini G (2003) Mode of action of *Ipomoea batatas* (Caiapo) in type 2 diabetic patients. Metabolism: Clinical and Experimental. https://doi.org/10.1016/S0026-0495(03)00073-8

Luo CL, Zhou Q, Yang ZW, Wang RD, Zhang JL (2018) Evaluation of structure and bioprotective activity of key high molecular weight acylated anthocyanin compounds isolated from the purple sweet potato (*Ipomoea batatas* L. cultivar Eshu No.8). Food Chemistry 241: 23–31. https://doi.org/10.1016/j.foodchem.2017.08.073

Markham KR (1989) Flavones, Flavonols and their Glycosides. https://doi.org/10.1016/B978-0-12-461011-8.50012-3

Matsui T, Ebuchi S, Kobayashi M, Fukui K, Sugita K, Terahara N, Matsumoto K (2002) Anti-hyperglycemic effect of diacylated anthocyanin derived from *Ipomoea batatas* cultivar ayamurasaki can be achieved through the α-glucosidase inhibitory action. Journal of Agricultural and Food Chemistry. https://doi.org/10.1021/jf025913m

Németh K, Plumb GW, Berrin JG, Juge N, Jacob R, Naim HY, Williamson G, Swallow DM, Kroon PA (2003) Deglycosylation by small intestinal epithelial cell β-glucosidases is a critical step in the absorption and metabolism of dietary flavonoid glycosides in humans. European Journal of Nutrition 42: 29–42. https://doi.org/10.1007/s00394-003-0397-3

Obi BC, Okoye TC, Okpashi VE, Igwe CN, Alumanah EO (2015) Comparative Study of the Antioxidant Effects of Metformin, Glibenclamide, and Repaglinide in Alloxan-Induced Diabetic Rats. Journal of Diabetes Research 2016: 1–5. https://doi.org/10.1155/2016/1635361

Ohkawa H, Ohishi N, Yagi K (1979) Assay for lipid peroxides in animal tissues by thiobarbituric acid reaction. Analytical Biochemistry 95: 351–358. https://doi.org/10.1016/0003-2697(79)90738-3

Olivas-Aguirre FJ, Rodrigo-García J, Martínez-Ruiz NDR, Cárdenas-Robles AI, Mendoza-Díaz SO, Álvarez-Parrilla E, González-Aguilar GA, De La Rosa LA, Ramos-Jiménez A, Wall-Medrano A (2016) Cyanidin-3-O-glucoside: Physical-chemistry, foodomics and health effects. Molecules 21: 1–30. https://doi.org/10.3390/molecules21091264

Ooi CP, Loke SC (2013) Sweet potato for type 2 diabetes mellitus. Cochrane Database of Systematic Reviews 2017. https://doi.org/10.1002/14651858.CD009128.pub3

Pandarekandy ST, Sreejesh PG, Thampi BSH, Sreekumaran E (2017) Hypoglycaemic Effect of Glibenclamide: A Critical Study on the Basis of Creatinine and Lipid Peroxidation Status of Streptozotocin-induced Diabetic Rat. Indian Journal of Pharmaceutical Sciences 79. https://doi.org/10.4172/pharmaceutical-sciences.1000290

Pottathil S, Nain P, Morsy MA, Kaur J, Al-Dhubiab BE, Jaiswal S, Nair AB (2020) Mechanisms of antidiabetic activity of methanolic extract of punica granatum leaves in nicotinamide/streptozotocin-induced type 2 diabetes in rats. Plants 9: 1–15. https://doi.org/10.3390/plants9111609

R Core Team (2019) R: A language and environment for statistical computing. R Foundation for Statistical Computing.

Rabbani SI, Devi K, Khanam S (2010) Protective role of glibenclamide against nicotinamide-streptozotocin induced nuclear damage in diabetic Wistar rats. Journal of Pharmacology and Pharmacotherapeutics 1: 18–23. https://doi.org/10.4103/0976-500X.64531

Rafi U AA, Luka CD (2018) Effects of aqueous extract of *Ipomoea batatas* Leaf on blood glucose, kidney functions and hematological parameters of streptozotocin-induced diabetic rats. J Res Diabetes Metab.

Rahajeng W (2015) Pendugaan keragaman karakter morfologi 50 aksesi plasma nutfah ubijalar. https://doi.org/10.13057/psnmbi/m010444

Schibli A, Reich E (2005) Modern TLC: A key technique for identification and quality control of botanicals and dietary supplements. Journal of Planar Chromatography - Modern TLC. https://doi.org/10.1556/JPC.18.2005.1.6

Song BJ, Sapper TN, Burtch CE, Brimmer K, Goldschmidt M, Ferruzzi MG (2013) Photo- and thermodegradation of anthocyanins from grape and purple sweet potato in model beverage systems. Journal of Agricultural and Food Chemistry 61: 1364–1372. https://doi.org/10.1021/jf3044007

Sun H, Zhang P, Zhu Y, Lou Q, He S (2018) Antioxidant and prebiotic activity of five peonidin-based anthocyanins extracted from purple sweet potato (*Ipomoea batatas* (L.) Lam.). Scientific Reports 8: 1–12. https://doi.org/10.1038/s41598-018-23397-0

Szkudelski T (2001) The mechanism of alloxan and streptozotocin action in B cells of the rat pancreas. Physiological Research 50: 537–546.

Truong V Den, Nigel D, Thompson RT, Mcfeeters RF, Dean LO, Pecota K V., Yencho GC (2010) Characterization of anthocyanins and anthocyanidins in purple-fleshed sweetpotatoes by HPLC-DAD/ESI-MS/MS. Journal of Agricultural and Food Chemistry 58: 404–410. https://doi.org/10.1021/jf902799a

Vessal M, Hemmati M, Vasei M (2003) Antidiabetic effects of quercetin in streptozocin-induced diabetic rats. Comparative Biochemistry and Physiology - C Toxicology and Pharmacology 135: 357–364. https://doi.org/10.1016/S1532-0456(03)00140-6

Vilhena RO, Figueiredo ID, Baviera AM, Silva DB, Marson BM, Oliveira JA, Peccinini RG, Borges IK, Pontarolo R (2020) Antidiabetic activity of Musa x paradisiaca extracts in streptozotocin-induced diabetic rats and chemical characterization by HPLC-DAD-MS. Journal of Ethnopharmacology 254: 112666. https://doi.org/10.1016/j.jep.2020.112666

Xiang W, Suo TC, Yu H, Li AP, Zhang SQ, Wang CH, Zhu Y, Li Z (2018) A new strategy for choosing "Q-markers" via network pharmacology, application to the quality control of a Chinese medical preparation. Journal of Food and Drug Analysis. https://doi.org/10.1016/j.jfda.2017.10.003

Zhao R, Li Q, Long L, Li J, Yang R, Gao D (2007) Antidiabetic activity of flavone from *Ipomoea batatas* leaf in non-insulin dependent diabetic rats. International Journal of Food Science and Technology 42: 80–85. https://doi.org/10.1111/j.1365-2621.2006.01215.x